2022

Anatomical Characterization of Descending Projections of Lateral Hypothalamic Glutamatergic and GABAergic Neurons

Jeremy Lesser
University of Connecticut, jeremy.lesser@uconn.edu

Anatomical characterization of descending projections of lateral hypothalamic glutamatergic and GABAergic neurons

Author: Jeremy Lesser, Physiology and Neurobiology, 2022 Holster Scholar
Mentor: Dr. Alexander Jackson, Department of Physiology and Neurobiology

Abstract

Important innate behaviors in mammals, such as sleep-wake regulation, arousal, eating, drinking, and stress, are associated with the lateral hypothalamic area (LHA). The LHA is a complex brain region consisting of broad populations of either excitatory glutamatergic neurons or inhibitory GABAergic neurons. Recent studies have revealed dense and heterogeneous fibers from both LHA populations projecting to neuromodulatory regions in the midbrain and brainstem, including the tuberomammillary nucleus (TMN), ventral tegmental area (VTA), dorsal raphe (DR), and locus coeruleus (LC). Viral tracing and immunohistochemistry were utilized to characterize the anatomy of LHA^{VGLUT2} and LHA^{VGAT} projections to the aforementioned regions in an effort to understand LHA regulation of innate behavior.

Introduction

The daily lives of all animals are characterized by specific sets of behaviors which direct normal physiology and are necessary to ensure survival. In mammals, many of these key behaviors, notably sleep-wake regulation, hunger, thirst, arousal, and stress, are coordinated by various structures in the brain and their corresponding neural circuits. One important brain structure for controlling these innate behaviors is the hypothalamus, which is common to all vertebrates. Disruptions to hypothalamic function have devastating effects on normal bodily functions. The specific hypothalamic neural circuits controlling each of these behaviors have not been sufficiently studied so more research is needed for their characterization and thus improve our understanding of these behaviors [15]. The lateral hypothalamic area (LHA) is a long structure comprising the lateral region of the hypothalamus and is itself in a central location of the brain where it interacts with many other systems utilizing numerous neural signaling pathways with long range projections [3]. Previous research has indicated that the LHA projects to major neuromodulatory regions within the brain which themselves regulate important innate behaviors, such as the tuberomammillary nucleus (TMN), ventral tegmental area (VTA), dorsal raphe (DR), and the locus coeruleus (LC) in addition to other regions [2].

Neurons within the LHA can be divided into two large populations, either neurons which utilize the fast excitatory neurotransmitter glutamate (LHA^{VGLUT2}) or those which utilize the fast inhibitory neurotransmitter gamma-aminobutyric acid (GABA) ($LHA^{VGAT)}$ [11]. Optogenetic behavioral assessments have revealed that LHA^{VGLUT2} neuron activation diminishes feeding and predatory behaviors [9, 14], while LHA^{VGAT} neuron activation enhances eating and reward-related behaviors [7, 12]. Additional studies in mice have shown that LHA^{VGAT} neuron activation also increases drinking and arousal [2] as well as wakefulness [5]. Single-cell RNA sequencing

of LHA neurons has identified 15 distinct clusters of LHA^{VGLUT2} neurons and 15 distinct clusters of LHA^{VGAT} neurons, suggesting that LHA neurons are highly heterogeneous [11]. Previous research has detailed two subpopulations of LHA^{VGLUT2} neurons, hypocretin/orexin neurons and melanin-concentrating hormone neurons, while little is known about the distinct subpopulations of LHA^{VGAT} neurons. Still more work is needed to understand the unique structure and function of these individual subpopulations of neurons within the LHA which may target different regions and promote different behaviors.

In this paper, LHA glutamatergic/GABAergic projections to the TMN, VTA, DR, and LC were examined using viral tracing and immunohistochemistry. This project utilized both anterograde and retrograde viral tracing. Anterograde tracing allows visualization of projections from the LHA to its downstream targets in the TMN, VTA, DR and LC, whereas retrograde tracing allowed us to visualize upstream to the regions that send projections to the LC. Specifically, this project focused on the LC and its surrounding structures within the pons, an area of the brainstem, which has been shown to receive dense LHA projections [13]. Anatomically, the LC is surrounded by four primary cell populations including Barrington's nucleus (Bar), the laterodorsal tegmental area (LDT), the pontine central gray (PCG), and the pre-LC (pLC) [1]. Bar is primarily composed of corticotropin-releasing hormone (CRH) neurons and is associated with urination and stress. The LDT consists of cholinergic neurons which have been shown to be associated with wake-state regulation and arousal. The PCG and pLC consist of FOXP2 expressing GABAergic neurons or glutamatergic neurons respectively which are structurally independent of the LC yet modulate its activity [8]. The aforementioned areas surrounding the LC can be visualized in Figure 1 below [17].

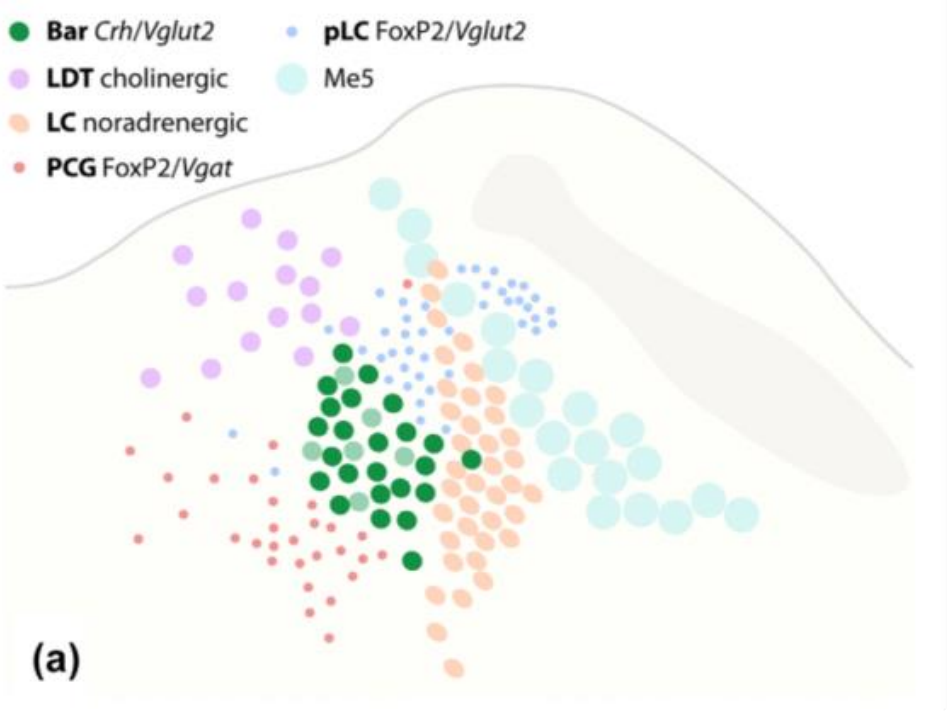

Figure 1: Neuron Populations Surrounding the Locus Coeruleus [17].

The LC itself consists of noradrenergic (LC^{NA}) neurons which have been associated with arousal, attention and stress, and have widespread projections throughout the entire central nervous system. Optogenetic stimulation of the LC has been associated with both increased wakefulness [4] and anxiety-like responses in mice [10]. Our knowledge of LHA^{VGLUT2} and LHA^{VGAT} projections to LC^{NA} and the surrounding structures are limited regarding the specific targets of these projections as well as the mechanisms by which they influence LC^{NA} activity. One possibility is that the LHA projects to the surrounding structures such as Bar and pre-LC, which in turn regulate the LC, however further experimentation is necessary to support this hypothesis.

This project was completed during the summer of 2022 with the help of Dr. Alexander Jackson's lab in the Department of Physiology and Neurobiology at the University of

Connecticut. All supplies and animals required for experimentation were provided by the Jackson lab. Funding for the project was generously donated by Mr. Robert Holster and Mrs. Carlotta Holster through the Holster Scholars program at the University of Connecticut.

Materials and Methods

Ethics Statements

All experiments were performed in accordance with the guidelines described in the National Institutes of Health Guide for the Care and Use of Laboratory Animals and were approved by the Institutional Animal Care and Use Committee of the University of Connecticut.

Mice

All mice were obtained from The Jackson Laboratory (Bar Harbor, ME) [16]. To isolate LHA glutamatergic neurons for analysis male and female *Slc17a6*/VGLUT2-cre mice were used. To isolate LHA GABAergic neurons for analysis male and female *Slc32a1*/VGAT-cre mice were used. For retrograde tracing, male and female VGAT-cre x Ai3 All mice were fed *ad libitum* and kept on a 12 h light-dark cycle.

Stereotaxic Injections

VGLUT2-cre/VGAT-cre mice received bilateral stereotaxic injections with a cre-inducible recombinant adeno-associated virus (AAV2) expressing the light-gated ion channel channelrhodopsin2 (ChR2), conjugated to an enhanced yellow fluorescent protein (EYFP) to visualize LHA^{VGLUT2}/LHA^{VGAT} neurons and their projections in green. Mice were bilaterally

injected with 30 nL of AAV2-EF1α-DIO-ChR2-EYFP virus directly into the LHA and incubated for 4 weeks before perfusion.

VGAT-cre x Ai3 mice received bilateral stereotaxic injections with cholera toxin B (CTB) virus to visualize LHA^{VGAT} neurons cell bodies in green and neurons projecting to the LC in red. Mice were bilaterally injected with 10 nL of CTB virus directly into the LC and incubated for 1 week before perfusion.

Immunohistochemistry

Jackson lab protocols were followed for all procedures. For IHC analysis, VGLUT2-cre and VGAT-cre mice were transcardially perfused with 10 ml 0.125 M NaCl, then 40 ml of a 1X phosphate buffered saline (PBS) solution containing 4% PFA. The dissected brains were postfixed overnight, then dehydrated in 30% sucrose for 48 h before being frozen in cold isopentane. Frozen brains were cut in coronal sections (anterior to posterior), 40 µm thick, on a cryostat (Leica CM3050 S). Sections were washed 2 x 5 min in 1X PBS, then washed 2 x 5 min in PBS and 0.2% Tween 20 (PBST). Sections were incubated in a blocking solution containing PBST and 2% donkey normal serum for 2 h at room temperature (RT). Sections were then incubated overnight at RT with mouse anti-tyrosine hydroxylase (TH, 1:1000, R&D Systems, catalog MAB7566), goat anti-cholera toxin B (CTB, 1:1000, List Labs, catalog 703), rabbit anti-tryptophan hydroxylase 2 (TPH2, 1:1000, Millipore, catalog ABN60), sheep anti-FoxP2 (1:1000, R&D Systems, catalog AF5647), goat anti-choline acetyltransferase (CHAT, 1:1000, Millipore, catalog AB144P). Sections were washed 5 x 10 minutes in PBST and then incubated with the appropriate secondary antibody raised in donkey conjugated to either Alexa Fluor 594, Alexa Fluor 488, or Alexa Fluor 405 (1:500, Abcam) in blocking solution for 2 h at RT. Sections were

washed 5 x 10 min in PBST and 5 x 10 min in PBS, then mounted onto slides with Vectashield hardset mounting media with or without DAPI (Vector Laboratories). Fluorescent imaging was performed using a Keyence BZ-X710. Confocal imaging was performed using a Leica SP8. Images were processed using Adobe Photoshop CS.

Results

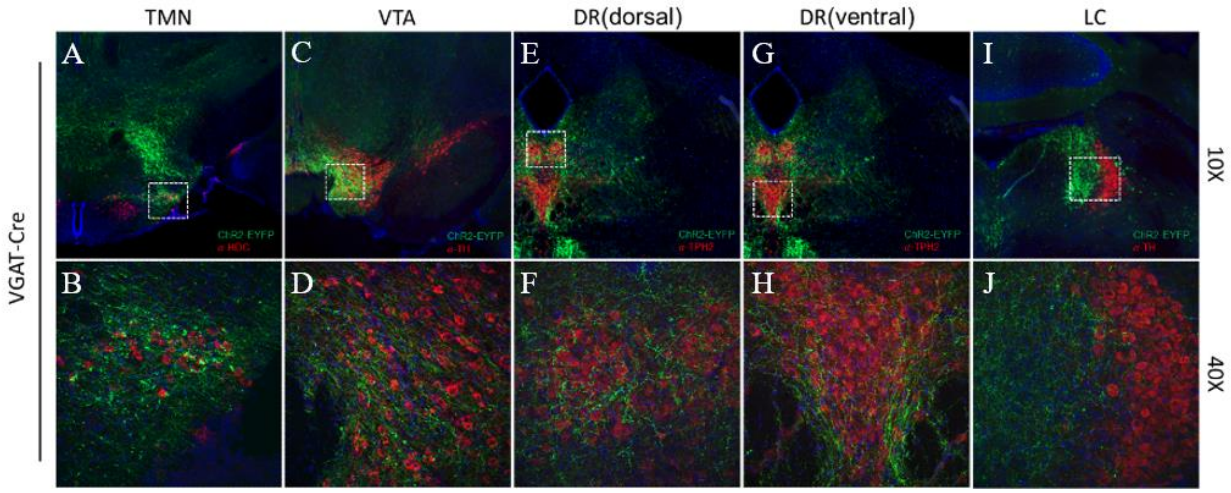

Figure 2: Anterograde tracing VGAT-cre projections from the LHA to the TMN, VTA, DR, and LC.

(A) ChR2-EYFP expressed selectively in fibers projecting to the TMN of a VGAT-cre mouse and immunofluorescence staining for histidine decarboxylase (HDC) in the TMN coronally sectioned. LHA^{VGAT} fibers (green) are in proximity to HDC+ cell bodies in the TMN (red). **(B)** Confocal images at 40X magnification of the TMN site showing HDC+ cell bodies in close proximity to EYFP+ fibers. **(C)** ChR2-EYFP expressed selectively in fibers projecting to the VTA of a VGAT-cre mouse and immunofluorescence staining for tyrosine hydroxylase (TH) in the VTA coronally sectioned. LHA^{VGAT} fibers (green) are in proximity to TH+ cell bodies in the VTA (red). **(D)** Confocal images at 40X magnification of the VTA site showing TH+ cell bodies in close proximity to EYFP+ fibers. **(E,G)** ChR2-EYFP expressed selectively in fibers projecting to the DR of a VGAT-cre mouse and immunofluorescence staining for tryptophan hydroxylase 2 (TPH2) in the DR coronally sectioned. LHA^{VGAT} fibers (green) are in proximity to TPH2+ cell bodies in the DR (red). **(F,H)** Confocal images at 40X magnification of the DR site showing TPH2+ cell bodies in close proximity to EYFP+ fibers. **(I)** ChR2-EYFP expressed selectively in fibers projecting to the LC of a VGAT-cre mouse and immunofluorescence staining for tyrosine hydroxylase (TH) in the LC coronally sectioned. LHA^{VGAT} fibers (green) are in proximity to TH+ cell bodies in the LC (red). **(J)** Confocal images at 40X magnification of the LC site showing TH+ cell bodies in close proximity to EYFP+ fibers.

***Images from Yi Huang**.

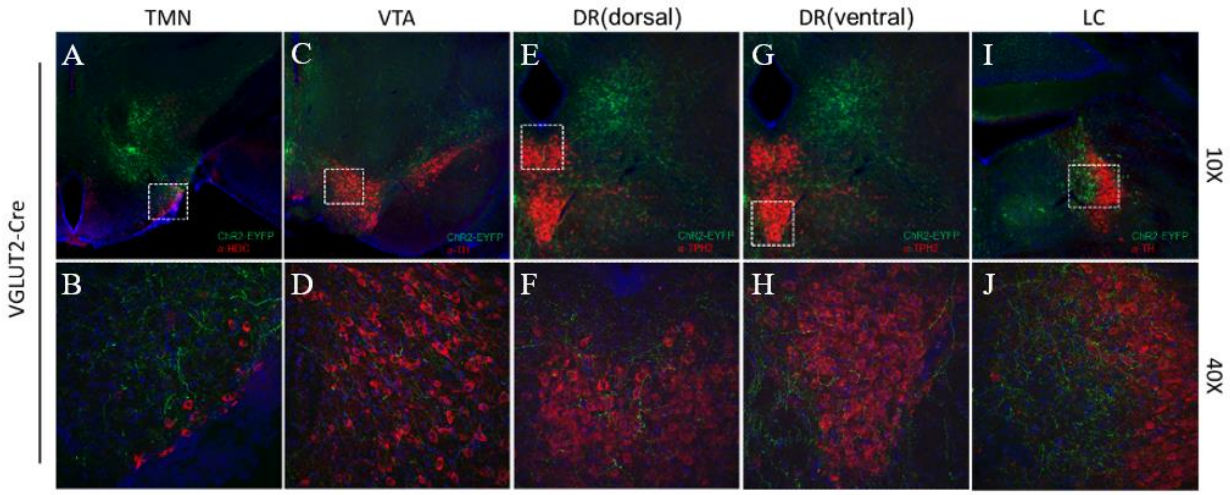

Figure 3: Anterograde tracing VGLUT2-cre projections from the LHA to the TMN, VTA, DR, and LC.

(A) ChR2-EYFP expressed selectively in fibers projecting to the TMN of a VGLUT2-cre mouse and immunofluorescence staining for histidine decarboxylase (HDC) in the TMN coronally sectioned. LHA^{VGLUT2} fibers (green) are in proximity to HDC+ cell bodies in the TMN (red). **(B)** Confocal images at 40X magnification of the TMN site showing HDC+ cell bodies in close proximity to EYFP+ fibers. **(C)** ChR2-EYFP expressed selectively in fibers projecting to the VTA of a VGLUT2-cre mouse and immunofluorescence staining for tyrosine hydroxylase (TH) in the VTA coronally sectioned. LHA^{VGLUT2} fibers (green) are in proximity to TH+ cell bodies in the VTA (red). **(D)** Confocal images at 40X magnification of the VTA site showing TH+ cell bodies in close proximity to EYFP+ fibers. **(E,G)** ChR2-EYFP expressed selectively in fibers projecting to the DR of a VGLUT2-cre mouse and immunofluorescence staining for tryptophan hydroxylase 2 (TPH2) in the DR coronally sectioned. LHA^{VGLUT2} fibers (green) are in proximity to TPH2+ cell bodies in the DR (red). **(F,H)** Confocal images at 40X magnification of the DR site showing TPH2+ cell bodies in close proximity to EYFP+ fibers. **(I)** ChR2-EYFP expressed selectively in fibers projecting to the LC of a VGLUT2-cre mouse and immunofluorescence staining for tyrosine hydroxylase (TH) in the LC coronally sectioned. LHA^{VGLUT2} fibers (green) are in proximity to TH+ cell bodies in the LC (red). **(J)** Confocal images at 40X magnification of the LC site showing TH+ cell bodies in close proximity to EYFP+ fibers. ***Images from Yi Huang**.

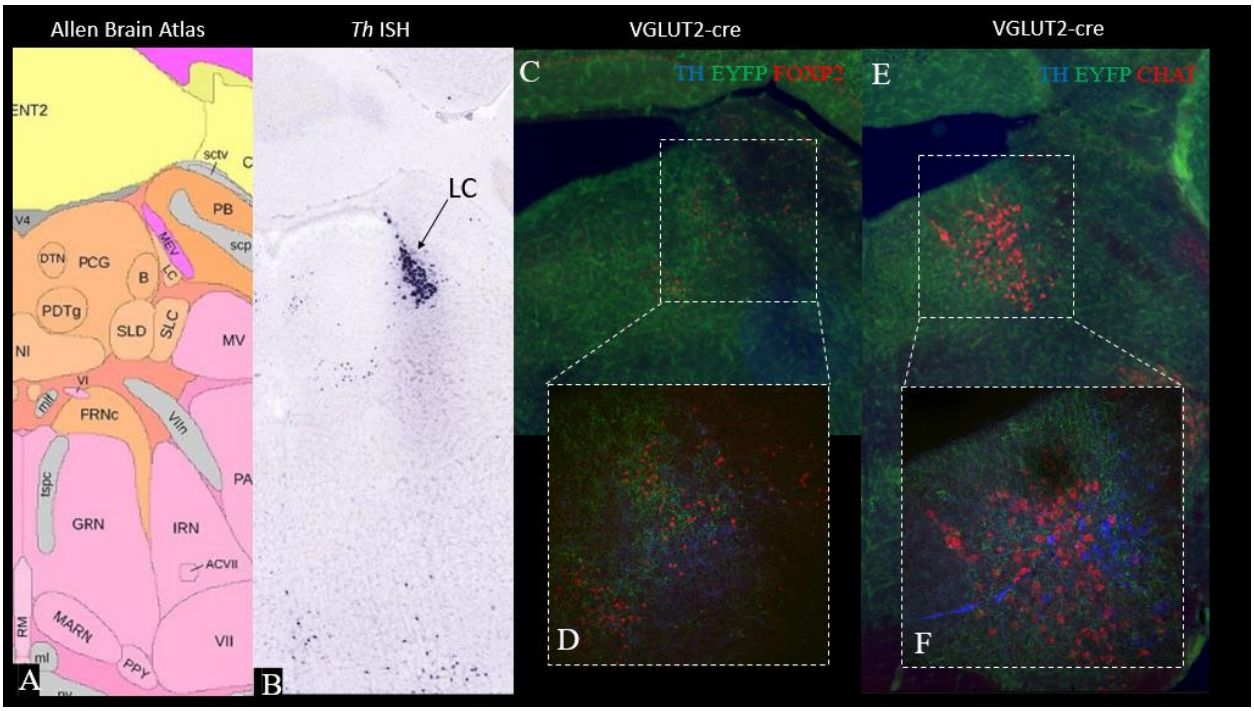

Figure 4: Anterograde tracing VGLUT2 projections from the LHA to the LC, PCG, pLC, and LDT. (A) Adult mouse coronal section showing the locus coeruleus (LC) from reference atlas [1]. **(B)** Adult mouse coronal section showing tyrosine hydroxylase (TH) ISH of the LC from reference atlas [1]. **(C)** ChR2-EYFP expressed selectively in fibers projecting to the LC of a VGLUT2-cre mouse and immunofluorescence staining for tyrosine hydroxylase (TH) and FoxP2 in the LC coronally sectioned. LHA^{VGLUT2} fibers (green) are in proximity to TH+ cell bodies in the LC (blue) and FOXP2+ cell bodies in the PCG and pLC (red). **(D)** Confocal images at 20X magnification of the LC site showing TH+ cell bodies and FOXP2+ cell bodies in close proximity to EYFP+ fibers. **(C)** ChR2-EYFP expressed selectively in fibers projecting to the LC of a VGLUT2-cre mouse and immunofluorescence staining for tyrosine hydroxylase (TH) and CHAT in the LC coronally sectioned. LHA^{VGLUT2} fibers (green) are in proximity to TH+ cell bodies in the LC (blue) and CHAT+ cell bodies in the LDT (red). **(D)** Confocal images at 20X magnification of the LC site showing TH+ cell bodies and CHAT+ cell bodies in close proximity to EYFP+ fibers.

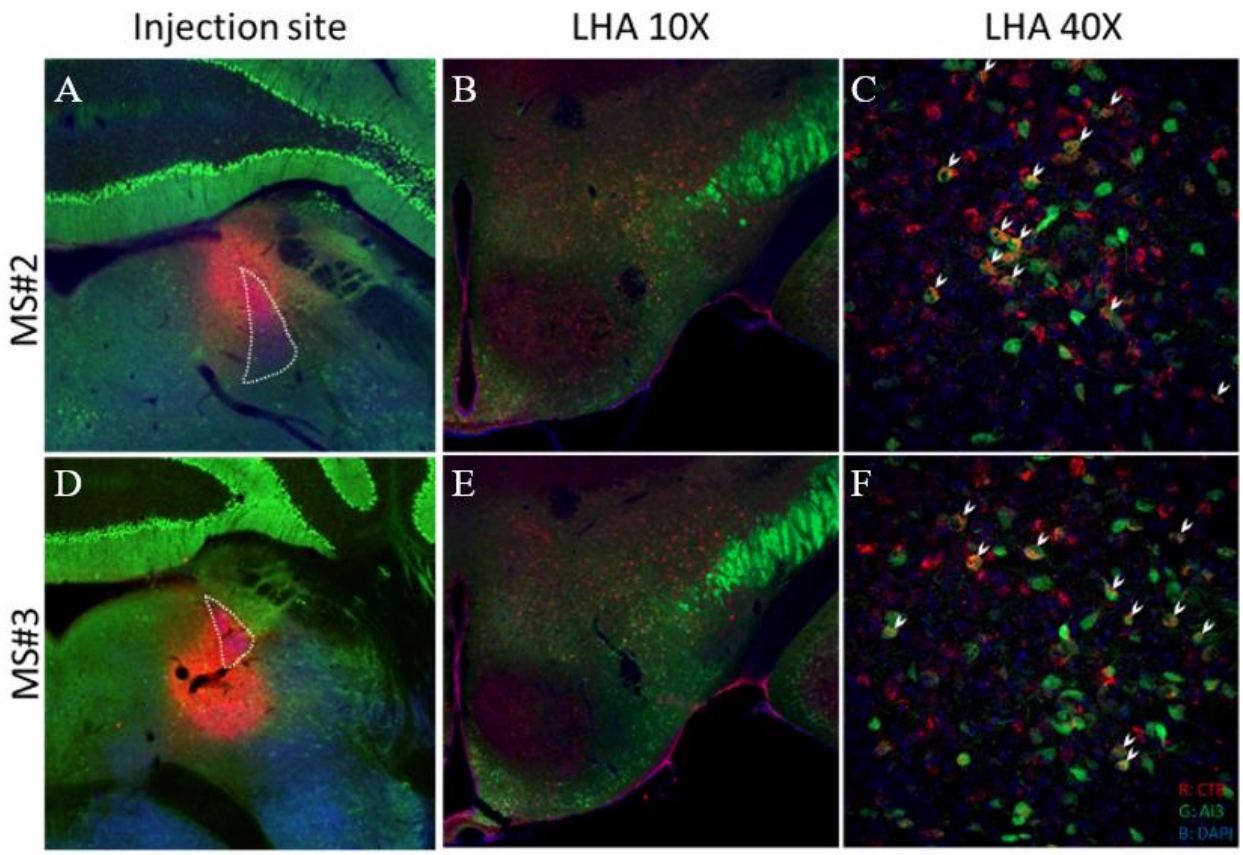

Figure 5: Retrograde tracing of VGABA projections from the LC to the LHA. (A) Adult mouse coronal section showing the injection site of MS#2 where 10 nL of CTB was injected into the LC of a VGAT-cre x Ai3 mouse. **(B,E)** CTB expressed in cell bodies which project to the LC from the LHA and immunofluorescence staining for CTB (red) and Ai3 (green), a GABAergic neuron cell marker, in the LHA coronally sectioned. CTB+ cell bodies (red) are colocalized with Ai3+ cell bodies (green) representing LHA^{VGAT} neurons projecting to the LC. **(C,F)** Confocal images at 40X magnification of the LHA site showing CTB+ cell bodies in close proximity to Ai3+ cell bodies. **(D)** Adult mouse coronal section showing the injection site of MS#3 where 10 nL of CTB was injected into the LC.

Discussion

Viral tracing and immunohistochemical analysis were utilized to examine the lateral hypothalamic GABAergic and glutamatergic projections to the TMN, VTA, DR, and LC.

LHA^{VGAT} projections were found to be strongly colocalized with HDC+ cell bodies of the TMN, TH+ cell bodies of the VTA, and TPH2+ cell bodies of the dorsal DR. LHA^{VGAT} projections were colocalized to a lesser degree with the TPH2+ cell bodies of the ventral DR and tended to be denser around the areas surrounding the ventral DR (Figure 2).

LHA^{VGLUT2} projections were found to be minimally colocalized with HDC+ cell bodies of the TMN and denser in the more dorsal region. LHA^{VGLUT2} projections were moderately colocalized with TH+ cell bodies of the VTA and TPH2+ cell bodies of the dorsal DR and strongly colocalized with the ventral DR (Figure 3).

Confocal microscopy revealed that LHA^{VGLUT2} projections were notably denser within the LC compared to LHA^{VGAT} projections, suggesting that LC^{NA} neurons receive primarily glutamatergic input from the LHA (Figure 3). LHA^{VGLUT2} and LHA^{VGAT} projections were both visualized to be dense in the surrounding areas of the LC, but not significantly within the LC itself. This suggests that LHA^{VGLUT2} and LHA^{VGAT} projections may regulate LC^{NA} neurons through modulation of structures near the LC, as previously hypothesized. Bar was shown to receive both LHA^{VGLUT2} and LHA^{VGAT} projections, revealing itself as a potential target of these lateral hypothalamic circuits (Figure 2). As expected, the pLC was defined by FOXP2+ cell bodies colocalizing with dense LHA^{VGLUT2} projections (Figure 4). The LDT, defined by CHAT+ cell bodies, was shown to have relatively weak colocalization with LHA^{VGLUT2} projections (Figure 4). LHA^{VGAT} projections to the PCG and LDT were unable to be visualized during this summer but will be examined in the future.

Figure 5 displays retrograde tracing from the LC to the LHA in which the presence of CTB+ signals represents that such cell bodies send projections to the LC and the presence of Ai3+ signals represents that such cell bodies are GABAergic. Imaging of the LHA revealed many distinct cell bodies with colocalized CTB (red) and Ai3 (green) signals which represent LHA^{VGAT} cell bodies which send projections to the LC and its surrounding structures. Cell bodies which only showed red signals represent non-GABAergic neurons within the LHA that project to the LC. Cell bodies which only showed green signals represent other LHA^{VGAT} cell bodies that do not project to the LC.

Conclusion

These images of LHA^{VGLUT2} and LHA^{VGAT} neuron projections to the TMN, VTA, DR, and LC further our understanding of the mechanisms in which the LHA controls its downstream targets and consequently, its control of behavior. The images suggested that both LHA^{VGLUT2} and LHA^{VGAT} neurons send projections to the TMN, VTA, and DR with LHA^{VGAT} projections typically colocalizing more with the cell bodies than LHA^{VGLUT2} projections. Imaging confirmed that both LHA^{VGLUT2} and LHA^{VGAT} neurons send distinct, dense projections to the structures surrounding the LC as well as few projections to the LC itself, highlighting multiple pathways in which the LHA can modulate behavior through LC^{NA} neurons. Retrograde tracing displayed specific LHA^{VGAT} neurons which project to the LC and its surrounding area. Additionally, immunohistochemical staining of the 15 subpopulations of glutamatergic or GABAergic neurons could reveal more specific connections within these projections. Visualization of images from some mouse sections and injection sites revealed, in some cases, either ineffective antibody staining or viral injection, invalidating the images of the sections. Further experiments could include additional mice to reduce the impact of these errors. Potentially utilizing fluorescence in

situ hybridization (FISH) staining instead of IHC staining could yield a strong comparison to these images as to visualize RNA instead of proteins.

Acknowledgements

I would like to thank Mr. Robert Holster and Mrs. Carlotta Holster for their generous donation that allowed me to explore my interest in research and neuroscience this summer. I would also like to thank Dr. Alexander C. Jackson for his continuous support throughout the entirety of my project, teaching me and answering all of my questions. I would also like to thank Yi Huang and the rest of the Jackson Lab for teaching me everything I would need to know to complete my project and guiding me through many new techniques. I would like to thank Dr. Vincent Moscardelli for being an incredibly supportive guide through the entire Holster Scholar process be it the application, classroom, or summer. Lastly, I would like to thank my Holster Scholar peers for being great friends and an amazing cohort to go through the Holster experience with.

Works Cited

[1] Allen Institute for Brain Science. (2006). Adult Mouse Brain Reference Atlas. Allen Brain Atlas. https://atlas.brain-map.org/

[2] Bonnavion, P., Mickelson, L. E., Fujita, A., de Lecea, L., & Jackson, A. C. (2016). Hubs and spokes of the lateral hypothalamus: cell types, circuits and behaviour. The Journal of Physiology, 58, 6443-6462.

[3] Brown, J. A., Woodworth, H. L., & Leinninger, G. M. (2015). To ingest or rest ? Specialized roles of lateral hypothalamic area neurons in coordinating energy balance. Frontiers in Systems Neuroscience, 9, 1–25.

[4] Carter, M. E., Yizhar, O., Chikahisa, S., Nguyen, H., Adamantidis, A., Nishino, S., Deisseroth, K., & de Lecea, L. (2010) Tuning arousal with optogenetic modulation of locus coeruleus neurons. Nature Neuroscience, 13, 1526–1533.

[5] Herrera, C. G., Cadavieco, M. C., Jego, S., Ponomarenko, A., Korotkova, T., & Adamantidis, A. (2015). Hypothalamic feedforward inhibition of thalamocortical network controls arousal and consciousness. Nature Neuroscience, 0–8.

[6] Huang, Y., Burleigh, E., Jackson, A. C. (2022). Neuroanatomical analysis of lateral hypothalamic GABAergic neuron projections and role in anxiety-like behavior. University of Connecticut.

[7] Jennings, J. H. H., Ung, R. L. L., Resendez, S. L. L., Stamatakis, A. M. M., Taylor, J. G. G., Huang, J... Stuber, G. D. D. (2015). Article Visualizing Hypothalamic Network Dynamics for Appetitive and Consummatory Behaviors. Cell, 160, 1–12.

[8] Jin, X., Li, S., Bondy, B., Zhong, W., Oginsky, M. F., Wu, Y., Johnson, C. M., Zhang, S., Cui, N., & Jiang C. (2016). Identification of a Group of GABAergic Neurons in the Dorsomedial Area of the Locus Coeruleus. PLoS ONE, 11 (1).

[9] Li, Y., Zeng, J., Zhang, J., Yue, C., Zhong, W., Liu, Z., Feng, Q., & Luo M. (2018). Hypothalamic Circuits for Predationa and Evasion. Neuron, 97, 911-924.

[10] McCall, J. G., Al-Hasani, R., Siuda, E. R., Hong, D. Y., Norris, A. J., Ford, C. P., & Bruchas, M. R. (2015). CRH engagement of the locus coeruleus noradrenergic system mediates stress-induced anxiety. Neuron, 87(3), 605-620.

[11] Mickelson, L. E., Bolisetty, M., Chimileski, B. R., Fujita, A., Beltrami, E. J., Constanzo, J. T., Naparstek, J. R., Robson, P., & Jackson, A. C. (2019). Single-cell transcriptomic analysis of the lateral hypothalamic area reveals molecularly distinct populations of inhibitory and excitatory neurons. Nature Neuroscience, 22, 642-656.

[12] Nieh, E. H., Matthews, G. A., Allsop, S. A., Presbrey, K. N., Leppla, C. A., Wichmann, R., Neve, R., Wildes, C. P., & Tye, K. M. (2015). Decoding Neural Circuits that Control Compulsive Sucrose Seeking. Cell, 160 (3), 528-541.

[13] Saper, C. B., Swanson, L. W., & Cowan, W. M. (1979). An autoradiographic study of the efferent connections of the lateral hypothalamic area in the rat. The Journal of Comparative Neurology, 183, 689–706.

[14] Stamanakis, A. M., Swieten, M. V., Basiri, M. L., Blair, G. A., Kantak, P., & Stuber, G. D. (2016). Lateral Hypothalamic Area Glutamatergic Neurons and Their Projections to the Lateral Habenula Regulate Feeding and Reward. The Journal of Neuroscience, 36(2), 302-311.

[15] Sternson SM (2013). Hypothalamic survival circuits: blueprints for purposive behaviors. Neuron. 77(5), p.810–824.

[16] The Jackson Laboratory. (n.d.). https://www.jax.org/

[17] Verstegen, A. M. J., Vanderhorst, V., Gray, P. A., Zeidel, M. L., & Geerling, J. C. (2017). Barrington's nucleus: Neuroanatomic landscape of the mouse "pontine micturition center". Journal of Comparative Neurology, 525 (10), 2287-2309.